Bioremediation of 1,4-Dioxane - Michigan Synthetic Biology Team

Introduction

1,4-Dioxane is a Group 2B Carcinogen and is a common byproduct of industrial processes[1]. As a cyclic ether, 1,4-dioxane does not break down easily and is prevalent in water sources and soil. Since the compound has been identified as possibly carcinogenic to humans, 1,4-dioxane poses an immediate risk to human health[2]. From 1966-1986, a medical device manufacturer improperly disposed of wastewater containing 1,4-dioxane into a tributary that feeds into the Huron River, the primary water supply for Ann Arbor, Michigan[3].

Ann Arbor is home to over 120,000 residents and is the location of our home institution, the University of Michigan, which enrolls nearly 50,000 students[4,5]. Currently there is a large groundwater plume containing 1,4-dioxane covering approximately 6 square miles, about 15.5 square kilometers, of the Ann Arbor area[6]. Despite over 30 years of cleanup efforts, the plume is actively spreading, threatening our community. 1,4-Dioxane does not stick to soil and migrates into groundwater with the potential to reach surface water[7]. There remain concentrations exceeding 85 parts per billion (ppb) and even reaching up to 2200 ppb in the plume[8]. These are concentrations over 300 times Michigan's legal limit of 7.2 ppb in residential drinking water, which was set by the state in 2017[9].

Currently, the status quo solution involves extraction wells that are used to bring up contaminated water to the surface. Then, ozone/hydrogen peroxide (O3/H2O2) advanced oxidation and UV irradiation are used to treat the contaminated water before release into the Huron River[10]. Due to this process being only 40-70% efficient and costing upwards of 1.2 million dollars per year, only one-eighth of the total 1,4-dioxane in the water supply had been removed as of 2019[10]. Furthermore, bromate, another likely human carcinogen, is released as a byproduct of the oxidation process[11]. As the 1,4-dioxane plume continues to spread through the groundwater of Ann Arbor, Scio Township, and surrounding areas, there exists an imminent threat to residents[12].

There is a need for a more efficient degradation process for 1,4-dioxane. Our solution capitalizes on the ability of genetically engineered aqueous bacteria to metabolize 1,4-dioxane with efficiency topping 55%[13]. Our proposed system of treatment involves synthetically modifying freshwater bacteria (Pseudomonas putida S16) to include a tetrahydrofuran monooxygenase gene (THFMO), first isolated from a bacteria found in industrial sludge and known to naturally degrade 1,4-dioxane[14]. We achieved this modification through the use of a plasmid vector containing the THFMO gene, an inducible arabinose promoter, and a gentamicin antibiotic resistance gene. Our team employed genetic engineering principles to degrade 1,4-dioxane in order to design a bioreactor supporting a groundwater treatment system for use in the affected communities.

Materials and Methods

Overview

This year's experimentation can be separated into four categories – separately transforming E. coli and P. putida to express THFMO, testing the degradation efficacy of THFMO of 1,4-dioxane for both host species, transforming P. putida to expressTHFMO, and testing the degradation of 1,4-dioxane with the THFMO construct

THFMO Construct and Transformation

The Bardwell lab at the University of Michigan provided a plasmid backbone containing NicA2, a nicotine metabolism gene, a gentamicin resistance gene, and strains of P. putida S16 and E. coli DH5α. We isolated the provided plasmid backbone via miniprep. Subsequent sequencing confirmed the successful isolation of the plasmid at its expected size of 10,309 bp. The EcoRI and XbaI restriction sites flanking the NicA2 gene were targeted by restriction enzyme digest to excise the gene. We confirmed the success of the restriction enzyme digest of our plasmid through gel electrophoresis, where we visualized two distinct bands at the expected sizes for the plasmid backbone and NicA2. To construct our THFMO-coding plasmid, we ordered the THFMO gene in three fragments from IDT, as this approach minimized the risk of mutations in the gene. These fragments would later be re-ligated through Gibson assembly to reform the fully functioning gene.

We began by performing PCR and subsequent PCR cleanup on the three fragments. We visualized the resulting samples through gel electrophoresis to confirm that each fragment was the expected size. We then used Gibson assembly to ligate the fragments and the plasmid vector backbone. Before transforming into P. putida, we transformed the Gibson product plasmid into E. coli to confirm the successful cloning through the Gibson reaction and possibly troubleshoot our protocol, as E. coli has a shorter doubling time (20 minutes versus 1.8 hours for P. putida) and is easier to transform. To transform into E. coli, we used heat shock transformation. We inoculated separate gentamicin plates with a negative control, positive control (for transformation), and our experimental sample.

A negative control was run, consisting of our restriction enzyme digested plasmid backbone with no Gibson assembly protocol performed and transformed into E.coli. This negative control would tell us how much background uncut plasmid would be in our Gibson reaction mixture. The positive control was the original backbone plasmid containing the nicotine metabolism gene transformed into E. coli. After seeing little growth on the negative control plate and substantial growth on the Gibson plate, we selected numerous colonies and extracted plasmid via miniprep. We then used gel electrophoresis to screen the sizes of these plasmids, since the THFMO containing plasmid should've been larger than the backbone. We then sequenced one of the possible Gibson plasmids to confirm that the experimental plasmid matched our theoretical THFMO containing plasmid.

Toxicity Assay

After successful transformation of the THFMO construct into both P. putida and E. coli, our first course of action was to ensure the bacteria could survive in an environment analogous to that of the degradation setting. As 1,4-dioxane is a carcinogenic substance, we decided to test bacterial growth of our transformed bacteria at various 1,4-dioxane concentrations. We set up overnight mini cultures of 10 mL LB media and a single colony from our transformation. Ten cultures were grown and each received a different concentration of 1,4-dioxane (0,1, 5, 10, 25, 50, 100, 250, 500, and 1000 ppm). Growth was measured via absorbance at 625 nm at t=0,16, 24, and 44 hours.

Initial Degradation Testing

Once we transformed the E. coli and P. putida, we cultured them to build up enough numbers for experiments and introduced dioxane to 10 mL samples to test degradation efficacy. As a requirement for expression, arabinose must be introduced into the cultures to induce the araBAD promoter in the plasmid. Consequently, we split the cultures into four experimental groups: transformed P. putida with arabinose, transformed P. putida without arabinose, untransformed P. putida with arabinose, and a final control solution with arabinose only. We performed the first set of experiments in LB Broth. Then we progressed to culturing in R2A media. R2A served as our minimal growth media, intended to reduce carbon sources outside of 1,4-dioxane for P. putida to use. We introduced 100 ppm of dioxane into each culture and took hourly time point samples, which were then stored at -80 ºC to prevent further degradation.

To monitor the growth of the bacteria, we measured the optical density of the cultures. To measure degradation, we used gas chromatography-mass spectroscopy (GC-MS). To prepare the GC-MS samples, we centrifuged our time point samples to remove any bacteria and solid waste from the sample. We then took 200 uL of the dioxane-containing supernatant and placed it into purified water vials. To reduce tailing, the samples were then diluted 1:30 by adding 10 uL sample to 290 uL millipore water. We then performed LLE, using DCM containing internal 1,4-dioxane standard as the organic phase which reduced variation in internal standard concentration as opposed to adding internal standard directly to samples. These samples were then held at -80 C to freeze the water layer to allow for the easy extraction of the dioxane-containing DCM layer.

Results

Overview

The first step of our experimentation involved transforming E. coli DH5α bacteria with a Tetrahydrofuran Monooxygenase (THFMO) gene derived from the Pseudonocardia dioxanivorans strain CB11901. A pJN105-NicA2 plasmid engineered with a nicotine metabolite gene (NicA2) in E. coli DH10β was obtained from the University of Michigan-affiliated Bardwell laboratory. First, we purified the plasmid via miniprep. Next, we used a restriction

enzyme digest to cut the NicA2 gene out of the acquired pJN105 backbone followed by a Gibson assembly to insert the THFMO gene (made of four subunits - thmA, thmD, thmB, and thmC into the plasmid)1. This new plasmid was heat-shocked into E. coli DH5α cells for glycerol stocks and possible controls in degradation experiments. Next, we used electroporation to transform into Pseudomonas putida S16, our final target bacteria for the bioreactor. After the successful transformation of P. putida S16, we tested 1,4-dioxane degradation via arabinose induced transformed P. putida (referred to as P. putida + THFMO) in R2A growth media spiked with 1,4-dioxane to closely resemble aquatic conditions. We used GC-MS to quantify dioxane concentrations, from which we determined that we were able to successfully degrade 1,4-dioxane at an efficiency of 58.591%.

Extract Original Plasmid

We grew overnight cultures of an E. coli DH10β strain containing the pJN105-NicA2 plasmid we obtained from the Bardwell lab. Via mini-prep, we extracted and purified the plasmid and then performed gel electrophoresis to validate its size (7494 bp), as seen in Figure 1. Sequencing later confirmed that we had the original, intact plasmid, as seen in Figure 2.

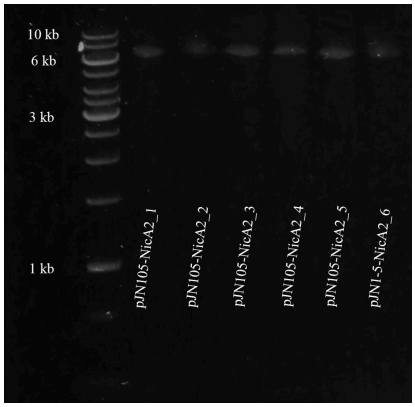

Figure 1. Gel electrophoresis of six different pJN105-NicA2 plasmids from E. coli colonies. Each plasmid ran around 7.5 kb as expected.

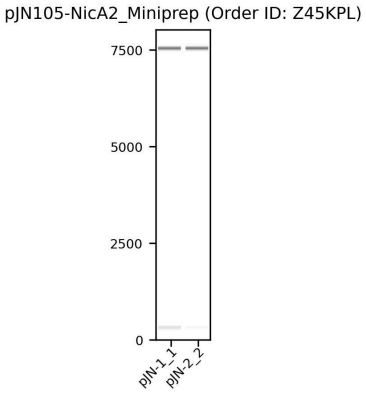

Figure 2. Sequencing done by Plasmidsaurus confirmed the extracted pJN105-NicA2 plasmid size and sequence. The received virtual gel from Plasmidsaurus is shown.

Remove Foreign Construct

The plasmid we obtained contained a nicotine metabolizing gene induced by arabinose and a gentamicin resistance cassette. The plasmid also had two restriction enzyme sites (EcoRI and XbaI) flanking the NicA2 insert. We

performed a restriction enzyme digest to remove the nicotine metabolizing gene from the plasmid backbone. To confirm that the RE digest was successful, we ran five digested samples on a gel, where we observed two separate bands for each lane: one for the digested plasmid backbone (~6 kb) and another for the nicotine gene fragment (~1.5 kb), as seen in Figure 3.

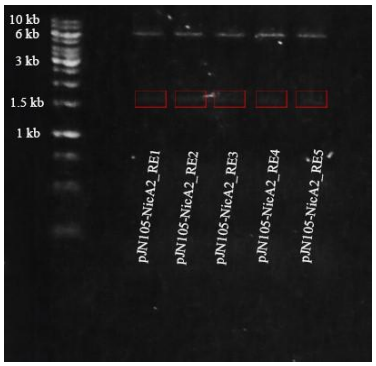

Figure 3. Restriction enzyme digest of the pJN105-NicA2 plasmid. We digested the plasmid with EcoRI-HF and XbaI enzymes. The 6 kb band is the backbone and the 1.5 kb band, boxed in red, is the NicA2 gene.

PCR THFMO Fragments

Since the THFMO gene is too large to be synthesized in one fragment without the risk of mutations, we obtained the THFMO gene from IDT split up into 3 fragments of lengths 915 bp, 2016 bp), and 1417 bp for a length of ~4.3 kb for the final assembled THFMO gene and used PCR to amplify the fragment concentrations.

Gibson Assembly

We proceeded with Gibson assembly to insert the THFMO sequence into our plasmid backbone for expression and cloning. This technique allowed us to insert the sequence isothermally, use relatively few reagents, and avoid restriction digest dependent ligations, which are prone to errors and tricky to execute with large fragments. We verified the successful insertion of the THFMO gene by running the experimental plasmid on a gel (expected length of 10.3 kb), as seen in Figure 4.

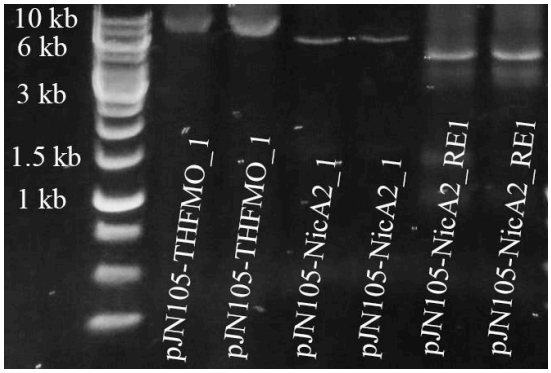

Figure 4. Gel electrophoresis of two Gibson-assembled pJN105-THFMO plasmids (Lanes 2 and 3), two original pJN105-NicA2 plasmids (Lanes 4 and 5), and two restriction enzyme digested pJN105-NicA2 plasmids (Lanes 6 and 7). Each plasmid ran at the expected length, being 10.3 kb for the pJN105-THFMO plasmids, 7.5 kb for the pJN105-NicA2 plasmids, and 6 kb + 1.5 kb fragments for the digested pJN105-NicA2 plasmids.

Transform E. Coli with THFMO Plasmid

Following the Gibson assembly of the THFMO sequence into the pJN105 plasmid backbone, we transformed the experimental pJN105-THFMO plasmid into E. coli via heat shock. Transformation success was verified by plating transformed bacteria onto a gentamicin agar plate, which would select only for bacteria that had successfully uptaken the pJN105-THFMO plasmid, since only bacteria containing the plasmid would express gentamicin resistance.

To verify our Gibson reaction's success, we screened the colonies that grew; this entailed growing a 5 mL LB culture of each of nine separate colonies theoretically containing pJN105-THFMO and then purifying the plasmid via miniprep followed by gel electrophoresis. Since the THFMO gene is 4.3 kb, the THFMO-containing plasmid should be noticeably larger and thus run slower on an agar gel. If the Gibson reaction was successful, pJN105-THFMO would be ~10.3 kb, whereas the original plasmid, pJN105-NicA2, was 7.5 kb. We determined three candidates for sequencing from the gel run due to visible plasmid banding at approximately 10.3 kb, as seen in Figure 5.

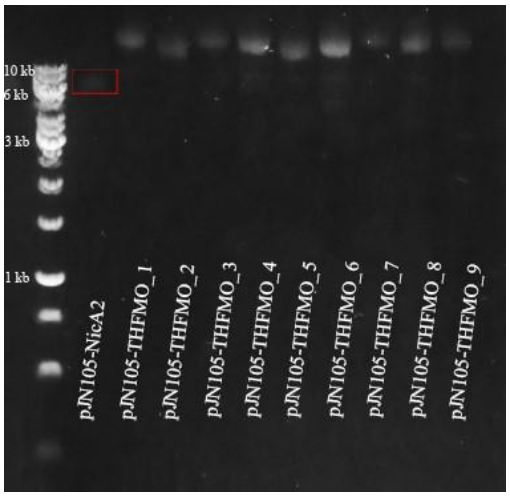

Figure 5. Gel electrophoresis of the original pJN105-NicA2 plasmid (Lane 2) as well as nine different transformed colonies' mini-prepped pJN105-THFMO plasmids (Lanes 3-11).

Upon observing that each colony migrated slower than the original pJN105-NicA2 plasmid and displayed variable positions on the gel, we decided to screen the first three mini-prepped plasmids further. These samples were located in Lanes 3, 4, and 5 of Figure 6. To achieve this, we amplified their THFMO inserts using PCR. For the amplification, we employed the forward Gibson primer of the THFMO fragment 1 and the reverse Gibson primer of the THFMO fragment 3. Once PCR was complete, we ran these amplified products on a gel, which yielded the gel in Figure 6.

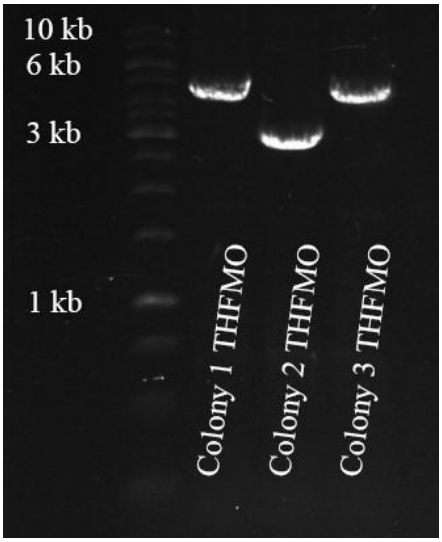

Figure 6. Gel electrophoresis of PCR amplified THFMO inserts from the three chosen experimental pJN105-THFMO plasmids (Lanes 3, 4, and 5 in Figure 5).

While the second plasmid in Figure 6 seems to lack at least one of the fragments of THFMO (later confirmed to be THFMO Fragment 2), the first and third plasmids have inserts between 4 and 5 kb, as expected. Knowing this, we confirmed the unaltered insertion of the THFMO sequence by sequencing all three plasmids of Figure 6, as seen in Figure 7.

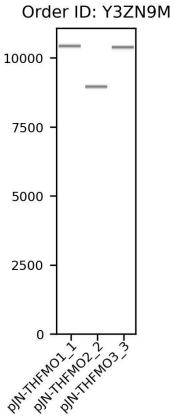

Figure 7. Sequencing by Plasmidsaurus confirmed that the third colony (Lane 5 from Figure 5) had the correct pJN105-THFMO size and sequence. The virtual gel received from Plasmidsaurus is shown.

Based on the gel and sequencing of our Gibson products, we had complete confidence in the success of our reaction. We confirmed that while the plasmid from lane 2 of Figure 5 had an extra duplication of an overlap region of the first THFMO fragment, the plasmid from lane 4 of Figure 5 had the correct, unaltered sequence (100.0% identity). We successfully confirmed the integrity of the THFMO gene, the arabinose-inducible promoter, and the gentamicin resistance gene. Thus, we decided to use this product for our future degradation testing.

Transform Putida with THFMO Plasmid

We transformed P. putida with the pJN105-THFMO plasmid via electroporation. Uptake by electroporation was necessary since the S16 strain of P. putida has been reported to have low efficiency with heat shock transformation. After electroporation, we screened for success as seen in Figure 8:

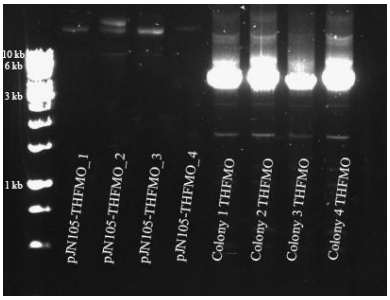

Figure 8. Gel electrophoresis of four P. putida S16 transformed colonies' mini-prepped pJN105-THFMO plasmids and PCR of their respective THFMO inserts.

From here, we decided to choose colony #3 for degradation experiments, seeing as the colony PCR had the least DNA "junk" in its lane (Lane 4 from Figure 8) and the amplified THFMO lane (Lane 8 Figure 8) did not have multiple strong extraneous bands.

Dioxane Degradation Testing with GC-MS

After confirming that 1,4-dioxane was not toxic to our bacteria, we tested its degradative efficiency. We created four biological replicate 10 mL cultures of each of three conditions in P. putida and one negative control absent of bacteria:

1. P. putida + THFMO + arabinose induction - This will check our experimental construct and see if 1,4-dioxane is being degraded.
2. P. putida + THFMO + no arabinose induction - This is to check for leaky expression of the araBAD promoter.
3. P. putida without a plasmid transformed + arabinose induction. - This is to check for natural uptake/degradation rates of dioxane.
4. A fourth technical replicate absent of bacteria was also created. - This is to check for evaporation rates of dioxane, which should be close to 1% according to calculations here.

Arabinose induction consisted of adding 0.02 w/v% of arabinose, 20 uL of 1 mg filtered arabinose per 10 mL water by weight, when cultures reached log phase at an OD of 0.8 at 600 nm (optimal phase for induction efficiency). We spiked each of these cultures with 100 ppm (mg/L), or 97.11 uL of 1:100 1,4-dioxane, at the same time as induction, and hourly 200 µL time point media samples were collected for the next 12 hours. Another time point was collected once daily over the second and third days of degradation. Immediately after collection, we froze the time point samples at -20C to stop degradation. Samples were prepared for GC-MS quantification to quantify their concentration of 1,4-dioxane. Figures 9-13 show degradation results:

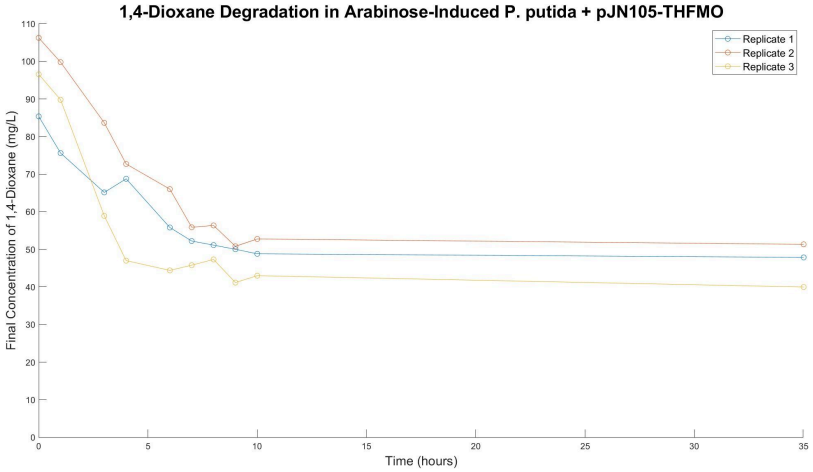

Figure 9. Degradation of 1,4-dioxane in arabinose-induced P. putida + THFMO bacteria over 12 hours.

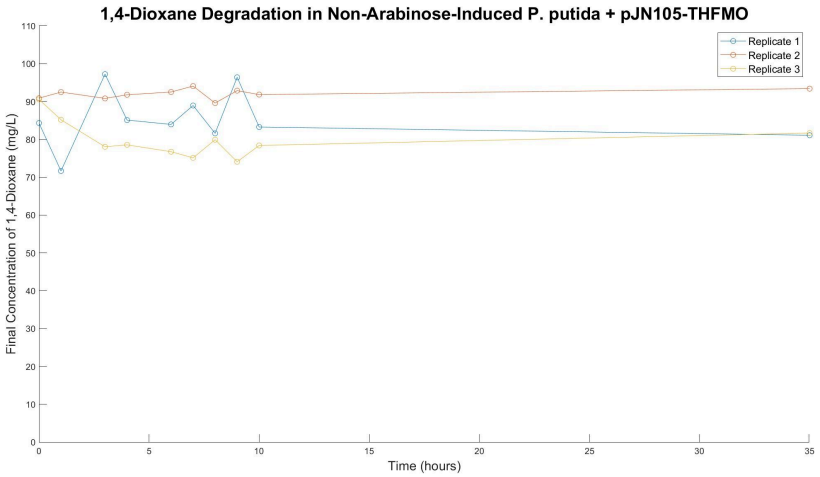

Figure 10. Degradation of 1,4-dioxane in non-arabinose-induced P. putida + THFMO bacteria (a control) over 35 hours.

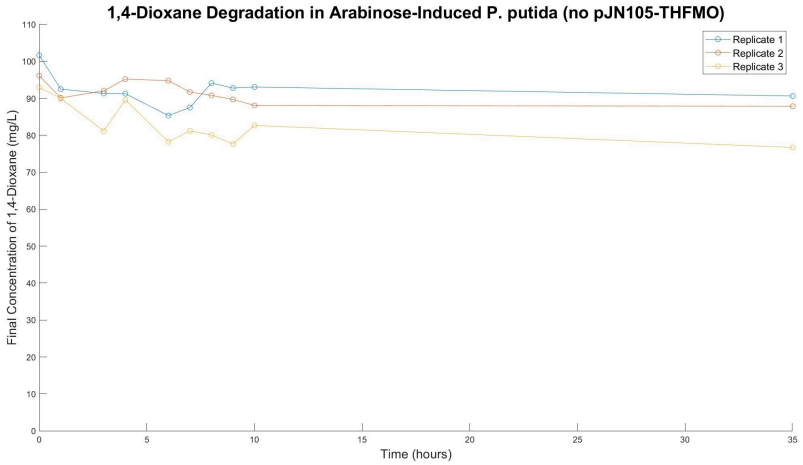

Figure 11. Degradation of 1,4-dioxane in arabinose-induced P. putida bacteria (a control) over 35 hours.

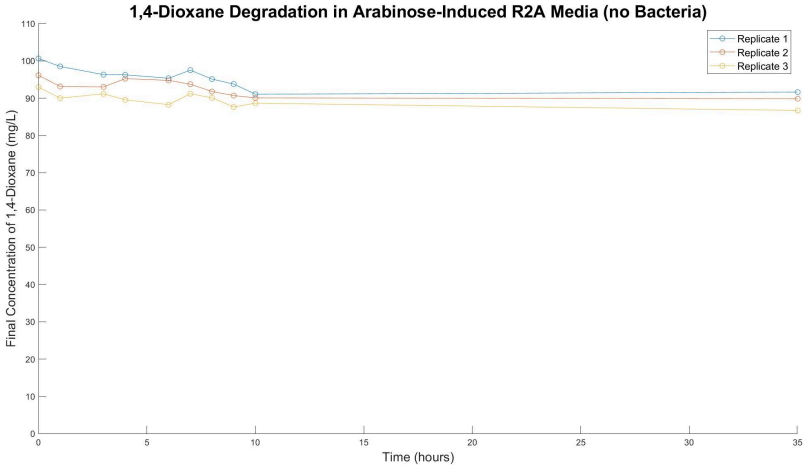

Figure 12. Degradation of 1,4-dioxane in arabinose-induced media with no bacteria (a control) over 35 hours.

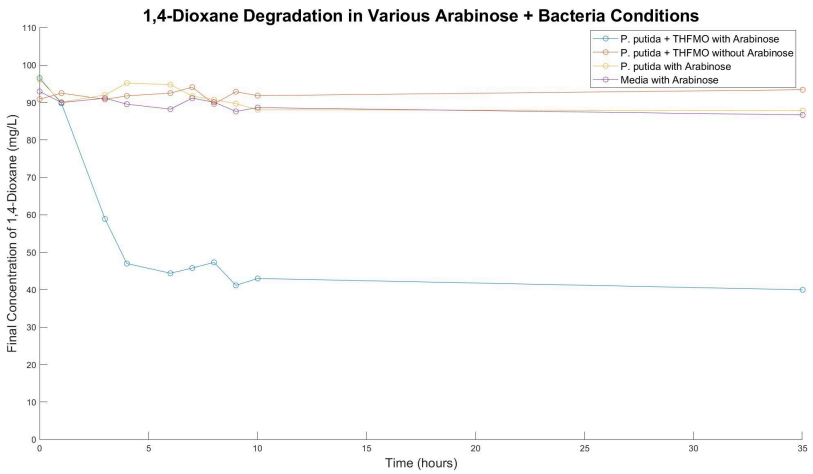

Figure 13. Comparison of degradation of 1,4-dioxane in media in various conditions over 35 hours.

Conclusion

Using the GC-MS Protocol, we quantified the 1,4-dioxane concentrations of our time point samples. The results (shown above) validate our model as a proof-of-concept for genetic engineering of P. putida S16 to express THFMO for its possible implementation in a bioreactor remediating 1,4-dioxane contamination. We believe the degradation efficiency of 58.592% is below our optimal degradation efficiency, as a plateau was observed, likely due to nutrient depletion, which would not occur in our bioreactor design. Additionally, our degradation occurred in an anaerobic environment (the only aeration was during time point sampling) and we would expect higher degradative efficiency in an aerobic bioreactor. As the current remediation method is 40-70% efficient, we believe our biodegradation system is a promising alternative which has the potential to improve efficiency and sustainability[2].

References

1. National Center for Biotechnology Information. PubChem Compound Summary for CID 31275, 1,4-Dioxane. PubChem. https://pubchem.ncbi.nlm.nih.gov/compound/1_4-Dioxane

2. Washtenaw County Health Department. 1,4-Dioxane. Washtenaw County, MI. www.washtenaw.org/1789/14-Dioxane

3. Ann Arbor City, Michigan. Explore Census Data, United States Census Bureau. 2020. https://data.census.gov/all?q=ann%20arbor

4. Campus Statistics. Students – Office of Budget and Planning, University of Michigan. 6 Oct. 2023. obp.umich.edu/campus-statistics/students/

5. 1,4 Dioxane. Huron River Watershed Council. 25 Oct. 2023. www.hrwc.org/our-watershed/threats/dioxane/

6. Loch-Caruso, R., Rayle, R., Caruso, V. P., Bailey, R. E., Collins, E., & Knol, K. P. (2022). Michigan's Gelman Site 1,4-Dioxane Groundwater Contamination: Still Spreading Decades after Detection. Current opinion in environmental science & health, 30, 100405. https://doi.org/10.1016/j.coesh.2022.100405

7. Huron River Watershed Council. Dioxane in Our Watershed. Huron River Watershed Council. https://www.hrwc.org/our-watershed/threats/dioxane/

8. Michigan Department of Environment, Great Lakes, and Energy. Gelman Sciences, Inc. Michigan.gov. https://www.michigan.gov/egle/about/organization/remediation-and-redevelopment/gelman-sciences-inc.

9. Michigan Department of Environment, Great Lakes, and Energy. Institutional Controls in Groundwater Management: 2024 Final Report. Michigan.gov. 2024. https://www.michigan.gov/egle/-/media/Project/Websites/egle/Documents/Offices/OGL/MGLPF/Final-Reports/Report-2024-Institutional-Controls-Groundwater-Management.pdf

10. Stanton Ryan. Ann Arbor Considering Worst-Case Scenario for Gelman Dioxane Plume. Mlive. 31 May 2019. www.mlive.com/news/ann-arbor/2019/05/ann-arbor-considering-worst-case-scenario-for-gelman-dioxane-plume.html.

11. Yang, Jingxin, et al. An Overview of Bromate Formation in Chemical Oxidation Processes: Occurrence, Mechanism, Influencing Factors, Risk Assessment, and Control Strategies. Chemosphere. vol. 237, 2019, 124521. https://doi.org/10.1016/j.chemosphere.2019.124521.

12. Loch-Caruso, Rita et al. Michigan's Gelman Site 1,4-Dioxane Groundwater Contamination: Still Spreading Decades after Detection. Current opinion in environmental science & health vol. 30 (2022): 100405. https://doi.org/10.1016/j.coesh.2022.100405

13. Zenker, M. J., Borden, R. C., & Barlaz, M. A. (2004). Biodegradation of 1,4-Dioxane Using Trickling Filter. Journal of Environmental Engineering. 130(9), 926–931. https://doi.org/10.1061/(ASCE)0733-9372(2004)130:9(926)

14. Wang, Peng, et al. Cometabolic Degradation of 1,4-Dioxane by a Tetrahydrofuran-Growing Arthrobacter sp. WN18. Ecotoxicology and Environmental Safety. vol. 217, 2021, 112206. https://doi.org/10.1016/j.ecoenv.2021.112206.

15. Laitner, Amy. Saline Gearing up for 3-Year, $62M Wastewater Treatment Plant Upgrades. MLive. 28 June 2023. www.mlive.com/news/ann-arbor/2023/06/saline-gearing-up-for-3-year-62m-wastewater-treatment-plant-upgrades.html

16. Sales, C. M., Grostern, A., Parales, J. V., Parales, R. E., & Alvarez-Cohen, L. (2013). Oxidation of the Cyclic Ethers 1,4-Dioxane and Tetrahydrofuran by a Monooxygenase in Two Pseudonocardia Species. Applied and Environmental Microbiology, 79. (24), 7702-7708. https://doi.org/10.1128/AEM.02418-13

17. Gelman Site of 1,4-Dioxane Contamination. ArcGIS web application. (2021). https://egle.maps.arcgis.com/apps/webappviewer/index.html?id=b2d077fdef2b4005883a5305a92ad1df

18. Grostern, A., Sales, C. M., Zhuang, W. Q., Erbilgin, O., & Alvarez-Cohen, L. (2012). Glyoxylate metabolism is a key feature of the metabolic degradation of 1,4-dioxane by Pseudonocardia dioxanivorans strain CB1190. Applied and environmental microbiology, 78(9), 3298–3308. https://doi.org/10.1128/AEM.00067-12

19. Database, A. P. S. (2022, November 1). Alphafold protein structure database. https://alphafold.ebi.ac.uk/entry/Q88CR0